

**1 Experimental study on the rate dependent strength**  
**2 of ice-silica mixture with silica volume fractions up to**  
**3 0.63**

Minami Yasui,<sup>1</sup> and Masahiko Arakawa<sup>1</sup>

---

M. Yasui, Graduate School of Environmental Studies, Nagoya University, Furo-cho, Chikusa-ku, Nagoya 464-8601, Japan. (yasui@eps.nagoya-u.ac.jp)

<sup>1</sup>Graduate School of Environmental Studies, Nagoya University, Japan.

4 We conducted deformation experiments of ice-1 $\mu$ m silica beads mixture  
5 to clarify the effect of silica beads volume fraction and temperature on the  
6 strength. The silica beads volume fraction was changed from 0 to 0.63 to sim-  
7 ulate the surface of icy bodies. Unconfined uniaxial compression tests were  
8 made in a cold room at the temperatures from -10°C to -25°C and the con-  
9 stant strain rates ranged from  $2.9 \times 10^{-3}$  to  $8.5 \times 10^{-7} \text{s}^{-1}$ . We determined the  
10 rate dependent strength of the mixture written by  $\dot{\epsilon} = A \cdot \sigma_{\max}^n$  from the  
11 relationship between the maximum stress,  $\sigma_{\max}$ , on the stress-strain curve  
12 and the applied strain rate,  $\dot{\epsilon}$ . The mixture with the silica volume fractions  
13 of 0.004-0.04 had almost the same strength with pure ice and the stress ex-  
14 ponent,  $n$ , is about 3. On the other hands, at the silica volume fractions more  
15 than 0.15, the mixture became harder as the beads were more included, and  
16 it had the same stress exponent, about 6. This high stress exponent might  
17 be caused by crack generation. Also, we found that the  $A$  for the silica vol-  
18 ume fractions more than 0.15 at -10°C was written by an exponential equa-  
19 tion related to the silica volume fraction,  $\phi$ ,  $A = 6.86 \times 10^{-8} \exp(-6.35\phi)$ .  
20 Furthermore, we found that the  $n$  of  $\phi=0.15$  was independent of the tem-  
21 perature, and the brittle-ductile boundary of  $\phi=0.29$  and 0.63 was more than  
22 30°C higher than that of pure ice.

## 1. Introduction

23 Water ice is distributed on the surfaces of Earth and Mars, and in many icy satellites  
24 of the outer solar system. It is revealed by recent planetary explorations that polar caps  
25 and layered deposits on Mars, and most of icy satellites have a rocky component in water  
26 ice, that is, they are composed of ice-rock mixture with various rock contents. Therefore,  
27 we must study the rheology of ice-rock mixtures to clarify the surface structures found on  
28 these extra-terrestrial bodies.

29 Brittle-ductile (B/D) boundary of ice-rock mixture is one of the most important rhe-  
30 ological properties to determine the tectonic style on the surface of icy bodies: various  
31 tectonic forces have deformed their surfaces to develop the geological structures related to  
32 brittle failure and ductile deformation such as faults and glacial flows. The experimental  
33 study on the B/D boundary of pure ice was made by *Schulson*[1990] and *Arakawa and*  
34 *Maeno* [1997], but that of the mixture has not been studied yet.

35 The rate dependent strength of ice-rock mixture has been studied in relation to ice  
36 engineering, glaciological interests and planetological implications. Previous studies re-  
37 ported that the mixtures of ice and solid particles became softer or harder than pure ice  
38 at small solid particles content, while did simply harder with increasing the content at  
39 large content. *Hooke et al.* [1972] and *Durham et al.* [1992] studied the strength or the  
40 viscosity of ice-sand mixture at the volume fractions from 0.0 to 0.6, and revealed that the  
41 mixture became weaker than pure ice as the volume fraction increased from 0 to 0.1-0.2,  
42 and above that, the mixture became harder.

43 *Mangold et al.* [2002] confirmed that the strength of ice-sand mixture at the volume  
44 fractions from 0.5 to 0.7 was about ten times larger than that of pure ice. They exper-  
45 imentally derived a flow law of ice-sand mixture, and the stress exponent showed 2.7,  
46 which was almost the same as that of polycrystalline water ice. The stress exponent is  
47 one of the most important factor to control the strength of the mixture. However, *Hooke*  
48 *et al.* [1972] and *Durham et al.* [1992] assumed the stress exponent, 3 or 4, to derive an  
49 enhancement factor of the flow law of ice-sand mixture. Thus, we must determine the  
50 stress exponent of the equation showing the rate dependent strength of ice-sand mixture  
51 experimentally, particularly we should study the dependence of sand content.

52 In this study, we carried out deformation experiments of ice-solid particles mixture sys-  
53 tematically to investigate the effects of solid particles on the B/D boundary and the stress  
54 exponent of the equation showing the rate dependent strength near the B/D boundary.

## 2. Experimental Methods

55 The sample of ice-solid particle mixtures was prepared by mixing ice grains with silica  
56 beads. Ice grains were produced by crashing commercial ice blocks into small pieces by  
57 using a blender. They were sieved to sort the grain size between 0.3 to 1mm. The silica  
58 beads have a smooth spherical shape with the diameter of  $1\mu\text{m}$  to exclude the effects of the  
59 shape and the size distribution of solid particle. It is widely accepted that the micron sized  
60 silicate dusts were very common in the solar nebula to be incorporated into icy bodies.  
61 Moreover, the surface of Mars is covered with micron sized dust that could be included  
62 in PLDs [*Neakrase et al.*, 2006]. We prepared the samples with the silica beads volume

63 fraction,  $\phi$ , of 0.004, 0.04, 0.15, 0.29, 0.49, and 0.63, and also did the polycrystalline ice  
64 sample without silica beads,  $\phi=0$ .

65 The sample preparation method is described as follows. At first, the ice grains are  
66 mixed with silica beads homogeneously. Then, a few amount of this mixed grains are put  
67 into a cylindrical mold and it is filled with liquid water at the temperature of  $0^{\circ}\text{C}$ . We  
68 repeat this process until the mixture fills the mold, and then freeze it in a cold room of  
69  $-10^{\circ}\text{C}$  for more than a day. We observed the sample texture by a microscope, and found  
70 that ice matrix which was the frozen water with silica beads was distributed among the  
71 ice grain boundaries. In the case of  $\phi=0.49$  and  $0.63$ , the preparation method is different  
72 from others: we pour the suspension of silica beads into the mold and then, freeze it. The  
73 sample has a cylindrical shape with the diameter of  $\sim 30\text{mm}$  and the height of  $\sim 60\text{mm}$ .  
74 There are unavoidable pores in the sample. The porosity before deformation was about  
75  $3\pm 2\%$ , and after deformation, it changed less than a few %, so the porosity has little effect  
76 on the strength.

77 We conducted unconfined uniaxial compression tests under constant strain rates by  
78 using the universal testing machine (TENSILON UCT-2.5). To examine the temperature  
79 dependence of the strength and the B/D boundary, we changed the cold room temperature  
80 from  $-10$  to  $-25^{\circ}\text{C}$ . The strain rates that we conducted in this experiment ranged from  
81  $2.9\times 10^{-3}$  to  $8.5\times 10^{-7}\text{s}^{-1}$ . We are especially interested in the stress exponent of the rate  
82 dependent strength, so that we made intensive tests at  $-10^{\circ}\text{C}$  to derive the dependence  
83 of the stress exponent on the silica volume fraction. Moreover, this temperature of -  
84  $10^{\circ}\text{C}$  and the unconfined condition are suitable for comparing our results with those of

85 *Mangold et al.*[2002] in order to study the effect of confining pressure, and these strain  
86 rates are suitable for comparing our results with that of *Durham et al.*[1992] obtained at  
87 low temperatures and high confining pressures.

### 3. Results and Discussions

#### 3.1. Deformation features

88 The stress-strain curves of the mixtures with different silica volume fractions at the same  
89 strain rate show the same trajectory before the stress reaches the maximum (auxiliary  
90 material Figure S1). Firstly, the stress linearly increases with the strain, and then the  
91 slope of the curve gradually approaches to zero, and the stress indicates the maximum.  
92 After the maximum, the stress decreases with increasing the strain, and then it becomes  
93 constant at small silica volume fractions, while it remains to decrease at large silica volume  
94 fractions. Moreover, at  $\phi=0.63$ , the stress decreases similarly but rises again at large  
95 strain. The rate dependent strength of ice was found to be expressed by the relationship  
96 between  $\dot{\epsilon}$  and  $\sigma_{\max}$  as follows [*Arakawa and Maeno, 1997*],

$$\dot{\epsilon} = A \cdot \sigma_{\max}^n, \quad (1)$$

97 where  $\dot{\epsilon}$  is the strain rate,  $\sigma_{\max}$  is the maximum stress, and  $A$  in the unit of  $\text{s}^{-1}(\text{MPa})^{-n}$   
98 and  $n$  are called as the flow parameters in this study. The rate dependent strength of ice  
99 in the ductile deformation without any crack generation is described by a creep flow law  
100 at low strain rates, however, near the B/D boundary, the deformation causes micro-cracks  
101 among grain boundaries even when ice is still ductile, and they might affect the strength.

102 *Sinha* [1988] theoretically constructed the rheological model of pure ice with micro-  
103 crack generation based on the elastic deformation and the creep flow law, and successfully  
104 applied the model to the deformation test at constant strain rates. Then, it showed that  
105 the stress exponent of Eq.(1) was almost the same as that of the creep flow law. Further-  
106 more, *Mellor and Cole* [1982] proposed that the rate dependent strength shown by Eq.(1)  
107 corresponded to the flow law constructed by creep tests when Eq.(1) was obtained by the  
108 unconfined compression test under a constant strain rate and near the B/D boundary.  
109 These previous studies pointed out the close relationship between the creep flow law and  
110 the rate dependent strength of pure ice. Then, we expect the same close relationship  
111 between them for the mixture hereafter.

### 3.2. Effects of silica beads volume fraction on the rate dependent strength

112 Figure 1 shows the relationships between the maximum stress and the strain rate of  
113 ice-silica beads mixtures with various silica volume fractions and pure ice at the constant  
114 temperature of  $-10^{\circ}\text{C}$ . The each data set with different silica volume fractions is shown  
115 in auxiliary material Table S1, and is fitted by Eq.(1). The fitted lines are shown on this  
116 figure for the reference.

117 At the silica volume fractions less than 0.04, the mixtures have almost the same strength  
118 as pure ice, that is, the maximum stresses become the same over the whole range of strain  
119 rates. However, at the silica volume fractions more than 0.15, the mixtures become harder  
120 as more silica beads are included, that is, the maximum stresses become larger as the silica  
121 volume fraction increases. As the strain rate increases, the difference of the maximum  
122 stress between pure ice and the mixture becomes smaller, in turn, the maximum stresses

of  $\phi=0.15-0.49$  are close to that of pure ice, about 3-4MPa at the strain rate of about  $10^{-4}\text{s}^{-1}$ . In the case of  $\phi=0.63$ , the maximum stress is larger than that of pure ice over the whole range of strain rates in this study. We notice that the order of the strength changes with the strain rates. This order is determined by the parameters of Eq.(1): they are the maximum stress on the fitted line at a standard strain rate,  $A$ , and the slope of the fitted line,  $n$ . So next, we examine the dependence of  $A$  and  $n$  on the silica volume fraction. The relationships of the silica volume fraction vs. the constant  $A$  or the power law index  $n$  are listed in Table 1.

### 3.2.1. Constant $A$

At the silica volume fractions less than 0.04, the  $A$  is almost same as that of pure ice. However, the  $A$  abruptly drops between 0.04 and 0.15, and then it decreases with increasing the silica volume fraction at more than 0.15. In the previous creep experiments of pure ice, the  $A$  represents the effect of temperature on the flow law, and also relates to the physical properties so called as enhancement factor, like crystal orientation, impurity contents and other factors [Paterson, 1994]. The enhancement factor, which is proportional to the  $A$ , caused by solid particles included in water ice has been measured by Durham *et al.* [1992] and it was found to be expressed by the exponential equation of the solid particles content. In this experiment, we found that the  $A$  exponentially decreased with increasing the silica volume fraction at more than 0.15. For example, the  $A$  for  $\phi=0.49$  becomes two orders of magnitude smaller than that of pure ice. So we fit these data by exponential equation and obtain as follows,



$$A = 6.86 \times 10^{-8} \exp(-6.35\phi). \quad (2)$$

144 The  $A$  represents the strain rate at 1MPa, so that we expect that the mixture can deform  
145 easily as the  $A$  becomes larger, although the actual strength also depends on  $n$ .

### 146 **3.2.2. Power law index $n$**

147 At the silica volume fractions less than 0.04, the  $n$  of the mixtures is almost constant  
148 of 3-4, which is same as that of pure ice. On the contrary, the  $n$  suddenly rises up from 3  
149 to 6 when the silica volume fraction changes from 0.04 to 0.15, and those of  $\phi=0.15-0.63$   
150 become almost constant, about 6.5.

151 These results are consistent with the results of previous works at the silica volume  
152 fractions less than 0.04 [*Hooke et al.*, 1972; *Durham et al.* 1992; *Mangold et al.*, 1999].  
153 They also concluded that the values of  $n$  with the solid particles volume fractions from  
154 0 to 0.04 were nearly equivalent with that of pure ice,  $n=3$ . However, our results are  
155 not consistent with previous results at the silica volume fractions more than 0.15. For  
156 example, *Li et al.* [2005] reanalyzed the results of *Hooke et al.* [1972] that the values of  
157  $n$  with the volume fractions from 0 to 0.6 decreased with increasing the volume fraction  
158 according to the equation of  $n = 3 - \phi$ . However, the  $n$  of our results increases with the  
159 silica volume fractions from 0.04 to 0.29, so are contrary to previous results. Additionally,  
160 the  $n$  of  $\phi=0.49$  of our result is twice as large as that of *Mangold et al.* [2002]: the  $n$  they  
161 obtained was about 2.7 which is equivalent to pure ice, while that we obtained was about  
162 7.

163 The result of *Mangold et al.* [2002] for the mixture of  $\phi=0.52$  is shown to compare  
164 with our result of  $\phi=0.63$  on Fig.1. The main difference of our experimental condition  
165 from that of *Mangold et al.* [2002] is a confining pressure. It is well known that the  
166 confining pressure reduces micro-crack generation and enhances the ductile deformation,  
167 so that we infer that the micro-cracks reduce the strength to cause the high values of  $n$  in  
168 our mixtures with large silica volume fractions. However, *Sinha* [1988] and *Arakawa and*  
169 *Maeno* [1997] showed that the micro-crack generation in pure ice did not change the stress  
170 exponent so much. According to *Sinha's* simulation, the number density of micro-crack  
171 was quite small until the stress achieved to the maximum, that means the maximum was  
172 caused by the ductile creep of ice, then the micro-cracks drastically increased to reduce the  
173 strength with increasing the strain. On the other hand, we speculate that at unconfined  
174 conditions the micro-cracks in the mixture might start to increase from the beginning of  
175 the deformation because of the strong stress concentration on silica inclusions, so that the  
176 confining pressure might strongly affect the stress exponent.

### 3.3. Effect of temperature on the rate dependent strength

177 The relationship between the maximum stress and the reciprocal of temperature with  
178 various silica volume fractions at the constant strain rate of  $1.4 \times 10^{-5} \text{s}^{-1}$  is shown in  
179 Fig.2, and auxiliary material Table S1. The maximum stress increases as the temperature  
180 becomes lower at each silica volume fraction, so we can fit these data by exponential  
181 equation. It is found that the slope of the line becomes larger as the silica volume fraction  
182 increases, that is, ice-silica mixture becomes more harder as the silica volume fraction  
183 increases. The data of  $\phi=0.15$  can be fitted by one exponential equation over the whole

184 range of temperature in this study, and furthermore at other strain rates, these data can  
 185 be fitted similarly.

186 We also examined the power law index  $n$  of  $\phi=0.15$  at the temperature lower than  $-10^{\circ}\text{C}$ ,  
 187 and the obtained  $n$  at different temperatures are listed in Table 1. It is found that the  $n$   
 188 is almost constant irrespective of the temperature. The fitted lines on Fig.2 are described  
 189 by the following equation according to the previous study on the rate dependent strength  
 190 [Arakawa and Maeno, 1997],

$$\sigma_{\max} = \left( \frac{\dot{\varepsilon}}{A_0} \right)^{1/n} \exp \left( \frac{Q}{nRT} \right), \quad (3)$$

191 where  $R$  is the gas constant, and  $T$  is the absolute temperature. According to Eq.(3), the  
 192 slopes of these lines are corresponding to  $Q/nR$ . Thus,  $Q/nR$  is derived to be  $6.4 \times 10^3$   
 193 for  $\phi=0.63$ ,  $3.9 \times 10^3$  for  $\phi=0.29$  and  $2.1 \times 10^3$  for  $\phi=0.15$ . We can calculate the activation  
 194 energy,  $Q$ , only for  $\phi=0.15$  by using the  $n$ , which was determined at the corresponding  
 195 temperature range: the average value was  $n=6.2$ . As a result, the  $Q$  is calculated to be  
 196  $129 \text{ kJ/mol}$  and is close to that of pure ice at the temperature higher than  $-8^{\circ}\text{C}$  [Barnes  
 197 *et al.*, 1971]. From this previous work, we know that the deformation mechanism of pure  
 198 ice at higher than  $-8^{\circ}\text{C}$  is grain boundary sliding among ice crystals. So, the deformation  
 199 mechanism of  $\phi=0.15$  may also be grain boundary sliding even at the temperature lower  
 200 than  $-10^{\circ}\text{C}$ .

201 We notice that in Fig.2 the deformation type of  $\phi=0.29$  and  $0.63$  changes from ductile  
 202 deformation to brittle failure as the temperature is  $-25^{\circ}\text{C}$ . Then, the maximum stress is  
 203 almost the same when the deformation type shows brittle failure. The deformation types

of  $\phi=0.29$  and  $0.63$  are shown on Fig.3, and in auxiliary material Table S1. The B/D boundary of these mixtures is proposed as follows [Arakawa and Maeno, 1997],

$$\dot{\epsilon}_{\text{bd}} = A_{\text{bd}} \cdot \exp\left(-\frac{E_{\text{bd}}}{RT}\right), \quad (4)$$

where  $A_{\text{bd}}$  is a constant of  $1.62 \times 10^{15} \text{ s}^{-1}$ , and  $E_{\text{bd}}$  is a constant of  $95.6 \text{ kJ/mol}$ . Comparing Eq.(4) with that of pure ice obtained by Arakawa and Maeno [1997], we can recognize that the boundary temperature is  $30\text{-}50^\circ\text{C}$  higher than that of pure ice at the same strain rate. Therefore, we expect that ice-silica beads mixtures with higher silica volume fractions could induce the brittle failure easily in comparison with pure ice, and this feature might correlate with many faults found on the surface of icy bodies such as Europa, Callisto and many Saturnian icy satellites.

**Acknowledgments.** We thank Prof. N. Azuma of Nagaoka University of Technology, for his useful advices and discussion and S. Nakatsubo of the Contribution Division of the Institute of Low Temperature Science, Hokkaido University, for his technical help. This work was partly supported by a grain-in-aid for scientific research (Grant 17340127) from the Japan Ministry of Education, Science, Sports, and Culture, and the Grant for Joint Research Program of the Institute of Low Temperature Science, Hokkaido University.

## References

Arakawa, M., and N. Maeno (1997), Mechanical strength of polycrystalline ice under uniaxial compression, *Cold regions science and technology*, *26*, 215–229.

- 221 Barnes, P., D. Tabor, and J. C. F. Walker (1971), The friction and creep of polycrystalline  
222 ice, *Proc. Roy. Soc. London, A324*, 127–155.
- 223 Durham, W. B., S. H. Kirby, and L. A. Stern (1992), Effects of dispersed particulates on  
224 the rheology of water ice at planetary conditions, *J. Geophys. Res.*, *97*(E12), 20883–  
225 20897.
- 226 Hooke, R. LeB., B. B. Dahlin, and M. T. Kauper (1972), Creep of ice containing dispersed  
227 fine sand, *J. Glacial.*, *11*, 327–336.
- 228 Li, H., M. S. Robinson, and D. M. Jurdy (2005), Origin of martian northern hemisphere  
229 mid-latitude lobate debris aprons, *Icarus*, *176*, 382–394.
- 230 Mangold, N., P. Allemand, P. Duval, Y. Geraud, and P. Thomas (1999), Ice content of  
231 martian permafrost deduced from rheology of ice-rock mixtures, *Lunar. Planet. Sci.*,  
232 *XXX*, Abstract 1016.
- 233 Mangold, N., P. Allemand, P. Duval, Y. Geraud, and P. Thomas (2002), Experimental and  
234 theoretical deformation of ice-rock mixtures: Implications on rheology and ice content  
235 of Martian permafrost, *Planet. Space Sci.*, *50*, 385–401.
- 236 Mellor, M., and D. M. Cole (1982), Deformation and failure of ice under constant stress  
237 or constant strain-rate, *Cold Regions Science and Technology*, *5*, 201–219.
- 238 Neakrase, L. D. V., R. Greeley, J. D. Iversen, M. R. Balme, and E. E. Eddlemon (2006),  
239 Dust flux within dust devils: Preliminary laboratory simulations, *Geophys. Res. Lett.*,  
240 *33*, L19S09, doi:10.1029/2006GL026810.
- 241 Paterson, W. S. B. (1994), *The physics of glaciers*, third ed., 85 pp., Elsevier, Oxford,  
242 UK.

- 243 Schulson, E.M. (1990), The brittle compressive fracture of ice, *Acta Metallurgica et Ma-*  
244 *terialia*, *30*, 1963–1976.
- 245 Sinha, N.K. (1988), Crack-enhanced creep in polycrystalline material: strain-rate sensitive  
246 strength and deformation of ice, *J. Mater. Sci.*, *23*, 4415–4428.

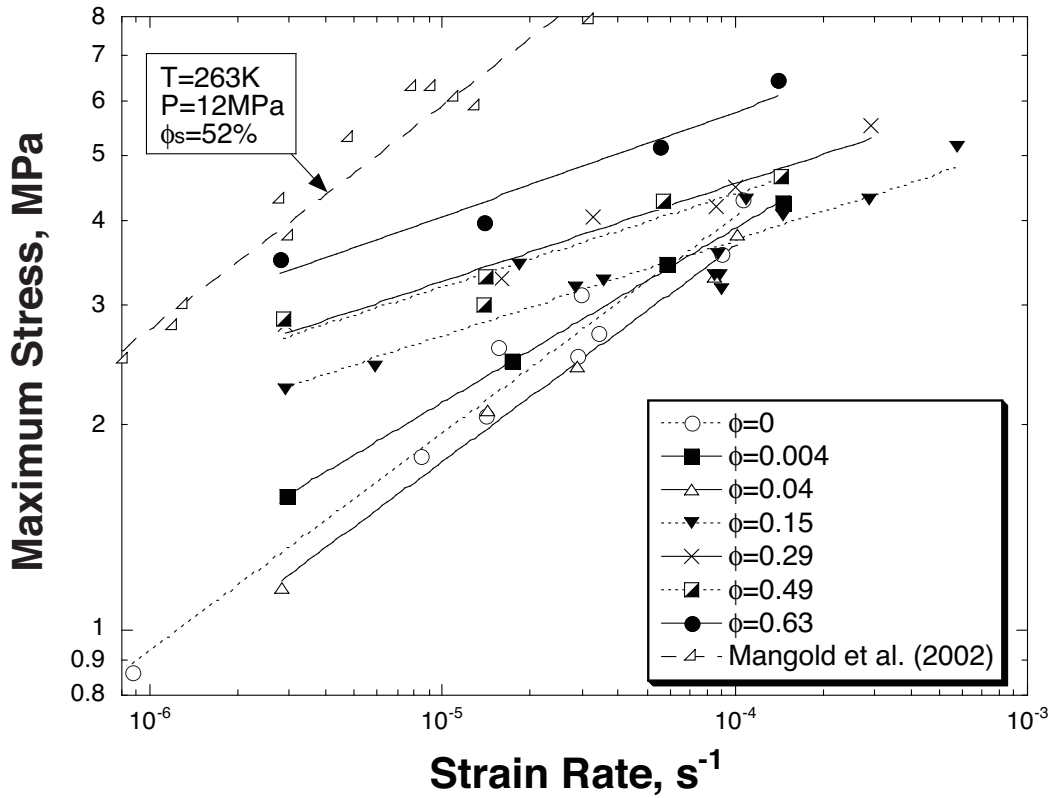


**Figure 1.** Maximum stress versus strain rate for pure ice sample (open circles) and ice- $1\mu m$  silica beads mixtures with the silica volume fractions of 0.004 (filled squares), 0.04 (open triangles), 0.15 (filled inverted triangles), 0.29 (X), 0.49 (half-filled squares), and 0.63 (filled circles) at the temperature of  $-10^{\circ}C$ . The lines are fitted by Eq. (1) at each silica volume fraction according to the least square method.

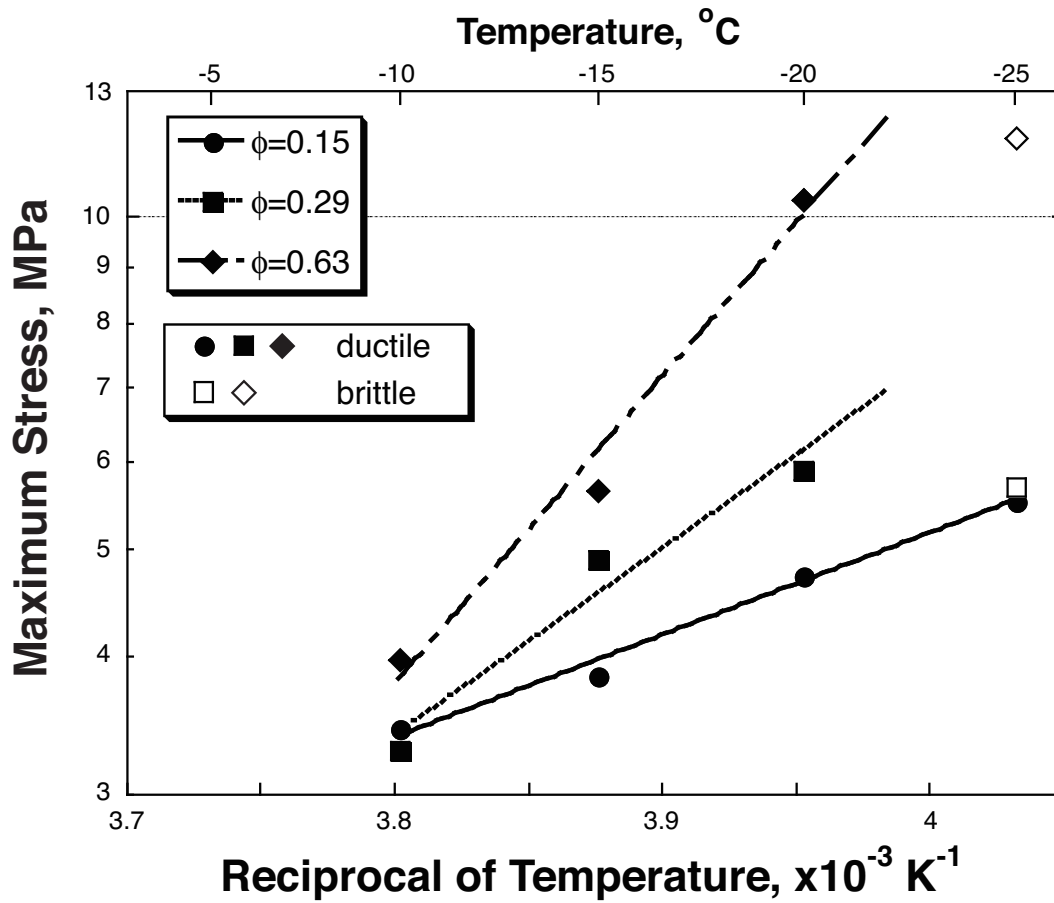


**Figure 2.** Temperature dependence of the strength for the mixtures with different silica volume fractions of 0.15, 0.29, 0.63. Filled symbols show ductile deformation, and open symbols show brittle failure.



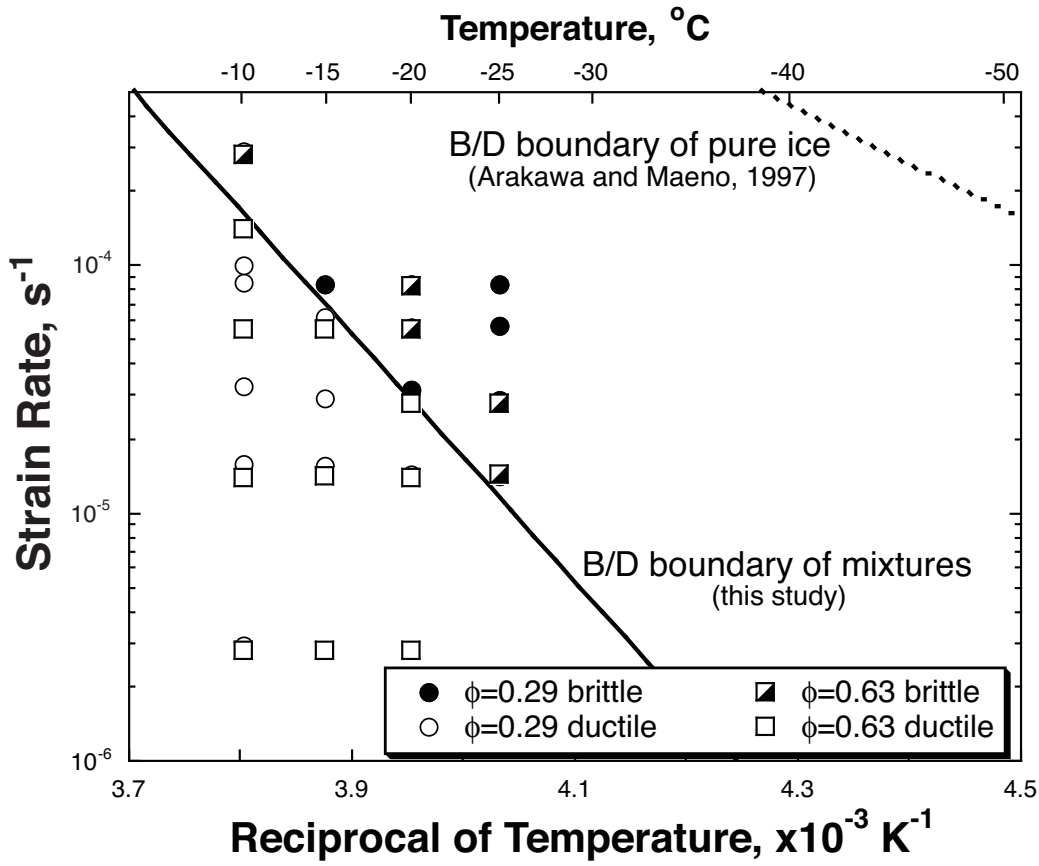


**Figure 3.** Deformation types of  $\phi=0.29$  and  $0.63$ . The previous result of the B/D boundary of pure ice is plotted by the dashed line [Arakawa and Maeno, 1997].

**Table 1.** Constant  $A$  and power law index  $n$  of Eq.(1)

Silica volume fraction, $\phi$	Temperature (°C)	$A$ ( $\text{s}^{-1}(\text{MPa})^{-n}$ )	$n$
0	-10	$1.35 \times 10^{-6}$	2.84 ( $\pm 0.25$ )
0.004	-10	$4.97 \times 10^{-7}$	3.90 ( $\pm 0.05$ )
0.04	-10	$1.70 \times 10^{-6}$	3.12 ( $\pm 0.18$ )
0.15	-10	$3.11 \times 10^{-8}$	6.05 ( $\pm 0.51$ )
0.15	-15	$1.24 \times 10^{-9}$	6.84 ( $\pm 1.21$ )
0.15	-20	$9.81 \times 10^{-10}$	6.37 ( $\pm 0.78$ )
0.15	-25	$8.98 \times 10^{-10}$	5.62 ( $\pm 0.45$ )
0.29	-10	$4.00 \times 10^{-9}$	6.67 ( $\pm 0.45$ )
0.49	-10	$5.02 \times 10^{-9}$	6.60 ( $\pm 0.84$ )
0.63	-10	$1.88 \times 10^{-9}$	6.15 ( $\pm 0.71$ )